


Nano-Encapsulation of Bilirubin in Pluronic F127–Chitosan Improves Uptake in β Cells and Increases Islet Viability and Function after Hypoxic Stress

Bronwyn Fullagar¹, Wei Rao², Chen Gilor¹, Feng Xu¹, Xiaoming He², and Christopher A. Adin³

Cell Transplantation
2017, Vol. 26(10) 1703–1715
© The Author(s) 2017
Reprints and permission:
sagepub.com/journalsPermissions.nav
DOI: 10.1177/0963689717735112
journals.sagepub.com/home/ctl


Abstract

Pancreatic islet transplantation is the only curative, noninvasive treatment for type 1 diabetes mellitus; however, high rates of cell death in the immediate postimplantation period have limited the success of this procedure. Bilirubin, an endogenous antioxidant, can improve the survival of murine pancreatic allografts during hypoxic stress but has poor solubility in aqueous solutions. We hypothesized that nano-encapsulation of bilirubin in pluronic 127–chitosan nanoparticle bilirubin (nBR) would improve uptake by murine pancreatic islet cells and improve their viability following hypoxic stress. Nano-bilirubin was synthesized, and drug release characteristics were studied *in vitro*. Cellular uptake of nBR was compared to free bilirubin (fBR) in an insulinoma cell line (INS-R3) model using confocal-like structured illumination microscopy. Next, C57BL/6 mouse islets were treated with concentrations of 0 to 20 μ M of nBR, fBR, or empty nanoparticle (eNP), prior to incubation under standard or hypoxic conditions. Islet viability and function were compared between treatment groups. Release of bilirubin was greatest from nBR suspended in protein-rich solution. Increased, selective uptake of nBR by INS-R3 cells was demonstrated. Cell death after hypoxic stress was significantly decreased in murine islets treated with 5 μ M nBR (18.5% \pm 14.1) compared to untreated islets (33.5% \pm 17.5%; $P = 0.019$), with reduction in central necrosis. Treatment group had a significant effect on glucose stimulation index [SI], ($P = 0.0137$) and islets treated with 5 μ M nBR had the highest SI overall. Delivery of bilirubin using pluronic F127–chitosan NP improves uptake by murine islets compared to fBR and offers dose-dependent protective effects following hypoxic stress.

Keywords

diabetes, islet, transplant, bilirubin, nanoparticle, encapsulation

Introduction

Pancreatic islet transplantation is a potential curative and minimally invasive cell therapy for diabetes. However, several hurdles remain before this therapy can be widely applied. Massive cell death due to isolation stress and hypoxia associated with the transplantation process causes loss of up to 70% of functional islets in the first 72 hours after implantation, prior to onset of the acquired immune response.¹ Hypoxic stress of islets leads to activation of natural factor κ B signaling pathways, expression of tissue factor (TF), release of interleukin 1 β (IL-1 β) from resident macrophages and downregulation of anti-inflammatory cytokines, such as interleukin 10 (IL-10).² These changes lead to upregulation of cell apoptotic pathways and release of further inflammatory mediators and chemotactic factors from islets, which attract host macrophages. Islet cell

necrosis and apoptosis also results in release of intracellular proteins (damage-associated molecular patterns [DAMPs]) that trigger an innate host immune response via toll-like

¹ Department of Veterinary Clinical Sciences, The Ohio State University, Columbus, OH, USA

² Department of Biomedical Engineering, The Ohio State University, Columbus, OH, USA

³ Department of Clinical Sciences, North Carolina State University, Raleigh, NC, USA

Submitted: February 2, 2017. Revised: March 24, 2017. Accepted: April 18, 2017.

Corresponding Author:

Christopher A. Adin, College of Veterinary Medicine, North Carolina State University, 1060 William Moore Dr., Raleigh, NC 27606, USA.
Email: caadin@ncsu.edu



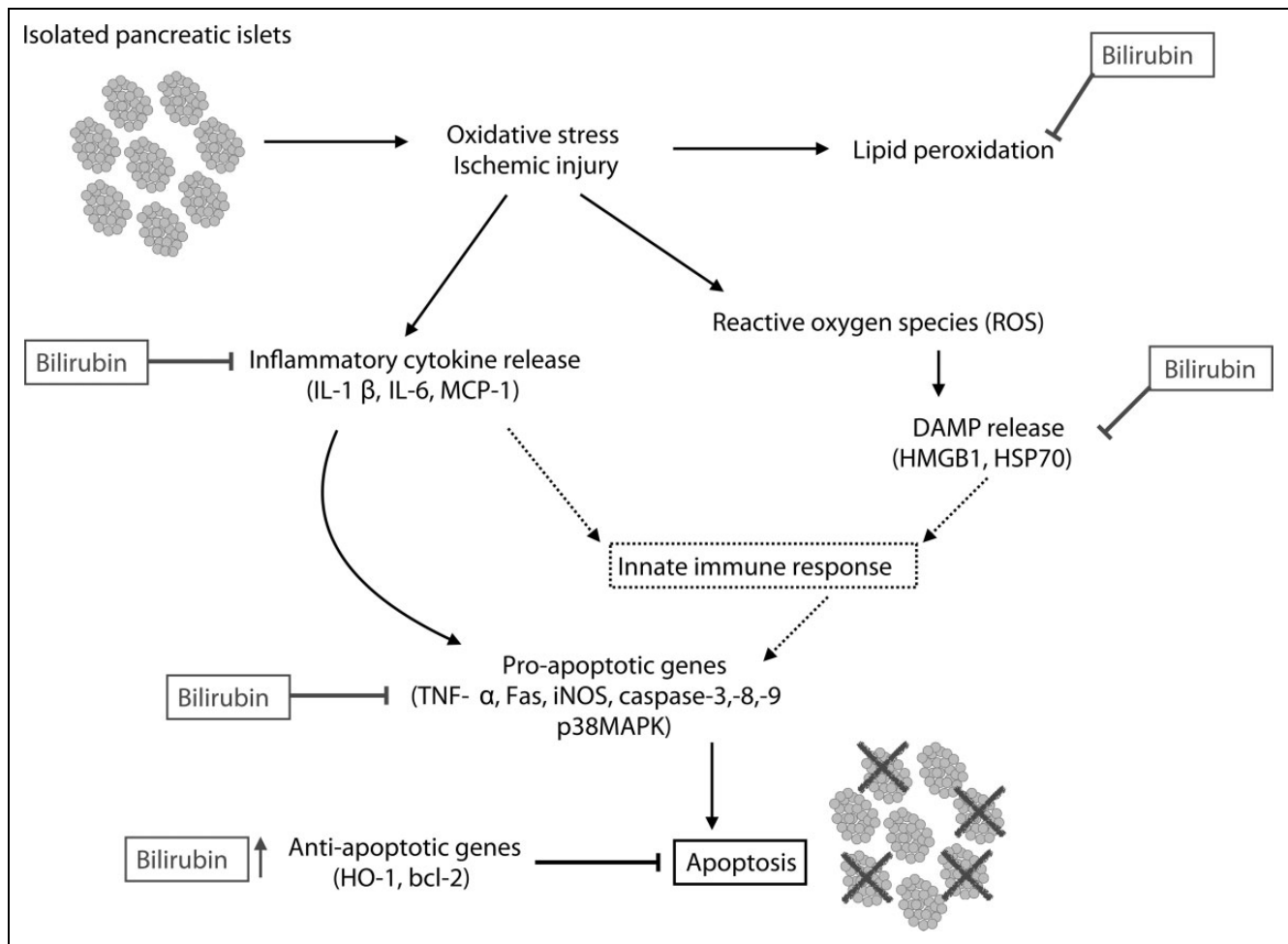


Figure 1. Cytoprotective properties of bilirubin. Bilirubin has been shown to intervene at multiple levels on the pathway to islet apoptosis.

receptor pathways. Cytokine release by host dendritic cells facilitates allorecognition and eventual allograft rejection.³

Bilirubin, a product of the enzyme heme oxygenase (HO-1), is a powerful antioxidant, with anti-inflammatory and cytoprotective properties that have been demonstrated in animal models of ischemia–reperfusion injury.⁴ Recent work by our group has shown that at therapeutic doses of 10 to 20 μM , bilirubin acts on islet grafts *in vitro* by suppressing the release of DAMPs and cytokines, resulting in significantly decreased cell death.⁵ Administration of bilirubin to murine pancreatic islet allograft recipients at doses of 10 to 20 μM significantly improved graft viability through attenuation of cell apoptosis and reduction in serum inflammatory mediators (IL-1 β , tumor necrosis factor alpha [TNF- α], soluble intercellular adhesion molecule-1 [sICAM-1], and monocyte chemoattractant protein-1 [MCP-1]).⁶ In addition, pretreatment of islet donors with 8.5 μM bilirubin significantly improved islet survival by upregulating expression of protective genes (HO-1 and bcl-2) and downregulating pro-inflammatory genes (MCP-1, caspase-3, caspase-8, TNF- α , and inducible nitric oxide synthase [iNOS]; Fig. 1).^{7,8} However, bilirubin is insoluble in water at physiologic pH,

is highly protein-bound in plasma, and has poor bioavailability, necessitating repeated intravenous or intraperitoneal administration.⁹ At higher concentrations, bilirubin is well known as a neurotoxin, particularly in susceptible newborns with neonatal jaundice. At concentrations above 25 μM , bilirubin has been shown to cross cell membranes and induce immunosuppression and apoptosis via mitochondrial depolarization.^{10,11} Thus, this molecule has a relatively narrow therapeutic range.

Polymeric nanoparticle (NP) drug delivery of hydrophobic compounds can improve solubility and bioavailability, reducing the effective drug dose and toxicity and allowing administration via the oral route. Pluronics are amphiphilic, triblock copolymers that form micelles in an oil-in-water emulsion, and pluronic F127 has been approved by the Food and Drug Administration (FDA) for use as a pharmaceutical ingredient.¹² Chitosan is a natural, biodegradable, cationic polysaccharide, found in the exoskeletons of crustaceans.¹³ Like pluronic F127, chitosan is amphiphilic and forms micelles by self-assembly when dispersed in water, with a hydrophobic core that can absorb hydrophobic molecules.¹⁴ Its positive surface charge facilitates penetration through

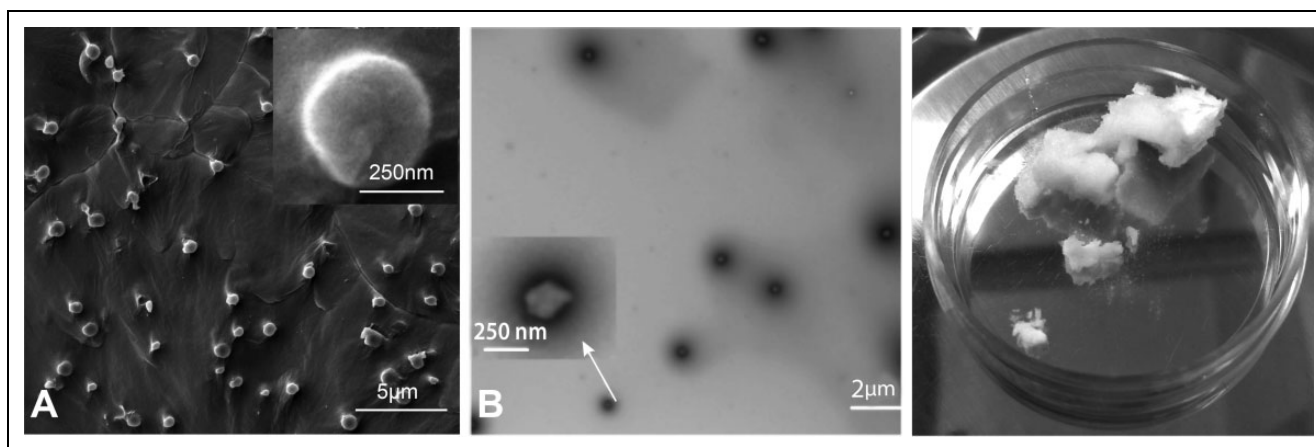


Figure 2. Microscopic and gross depictions of Pluronic F-127 chitosan nanoparticles (NP) and nanoencapsulated bilirubin synthesized for this study. (A) Scanning electron micrograph of empty Pluronic F-127 chitosan NP (eNP) at room temperature. NP are 293 nm at 22 °C (Adapted with permission from Rao W. et al.¹⁶ Chitosan-Decorated Doxorubicin-Encapsulated Nanoparticle Targets and Eliminates Tumor Reinitiating Cancer Stem-like Cells. *ACS Nano*. 2015; 9(6):5725-40. Copyright (2015) American Chemical Society.); (B) Transmission electron micrograph of Pluronic F-127 chitosan NP at room temperature; (C) Dry nanoencapsulated bilirubin (nBR) at room temperature (feeding ratio 1:20). nBR are 355 nm at 22 °C.

cellular membranes as well as adhesion to mucus glycoproteins.^{14,15} Pluronic F127–chitosan polymeric NPs have been shown to be highly stable and effective in the delivery of other hydrophobic molecules.¹⁶

We hypothesized that delivery of bilirubin via pluronic F127–chitosan NPs would allow for sustained drug release and improved drug uptake into pancreatic islet cells in culture when compared to free bilirubin (fBR). We further hypothesized that nanoparticle bilirubin (nBR) would improve the viability and function of isolated murine islets following exposure to hypoxic stress compared to unencapsulated bilirubin (fBR) or control.

Materials and Methods

Materials

Pluronic F127 (MW: 12.6 kDa) was obtained from BASF Corp (Wyandotte, Michigan, USA). Chitosan oligosaccharide of pharmaceutical grade (MW: 1.2 kDa, 95.5% deacetylation) was purchased from Zhejiang Golden-Shell Biochemical Co. Ltd (Zhejiang, China). Bilirubin (bilirubin-mixed isomers B4126; Sigma Aldrich, St Louis, Missouri, USA) stock solution of 1.29 mM at pH 7.4 was created by the following method: 0.2 N NaOH was added, dropwise, to 0.0584 g bilirubin powder. After dissolution of the bilirubin in NaOH, 40 mL Roswell Park Memorial Institute Media (RPMI 1640) without phenol red with 10% fetal bovine serum (FBS) was added. The pH was adjusted to 7.4 by gradual addition of HCl. Further RPMI + 10% FBS was added to yield a total volume of 50 mL. The solution was filtered, then the concentration of bilirubin was measured using the colorimetric diazo method (Cobas c311 Analyzer, Roche Diagnostics, Rotkreuz, Switzerland).

Synthesis of Pluronic F127–chitosan Nanoparticles

Pluronic F127–chitosan NPs with a core-shell architecture were synthesized using a previously reported method^{12,16} with slight modification. Briefly, a total of 30 mL of pluronic F127 solution (26 mM in benzene) was added drop wise into 30 mL of 4-nitrophenyl chloroformate (4-NPC) solution (160 mM in benzene), and the mixture was stirred for 3 h in N₂ atmosphere at room temperature to activate pluronic F127. The activated polymer was precipitated and filtered in excess (ice-cold) diethyl ether 3 times, then dried overnight under vacuum conditions. To synthesize pluronic F127–chitosan NPs, a total of 500 μL of the activated polymer (300 mg/mL or 23.2 mM) in dichloromethane was added dropwise into 5 mL of chitosan solution (15 mg/mL or 12.5 mM) in deionized (DI) water at pH 10 under sonication using a Branson 450 digital sonifier (Danbury, Connecticut, USA) at 16% of maximum amplitude for 3 min. Dichloromethane was then removed by rotary evaporation. The resultant solution was dialyzed against DI water with a Spectra/Por (Spectrum Laboratories, Houston, Texas, USA) dialysis tube (MWCO, 50 kDa) overnight and further dialyzed against DI water for 3 h using 1000 kDa Spectra/Por dialysis tube. Finally, the sample was freeze-dried for 48 h to obtain dry NPs. The resultant NPs are ~20 nm at 37 °C (Fig. 2A and B).¹⁶

Encapsulation of Bilirubin to Obtain Nanoparticle-encapsulated Bilirubin

Bilirubin was encapsulated in the pluronic F127–chitosan NPs using a method reported elsewhere.¹⁶ Briefly, 20 mL of bilirubin solution in chloroform (0.25 mg/mL) was added dropwise into 10 mL of aqueous solution (10 mg/mL) of

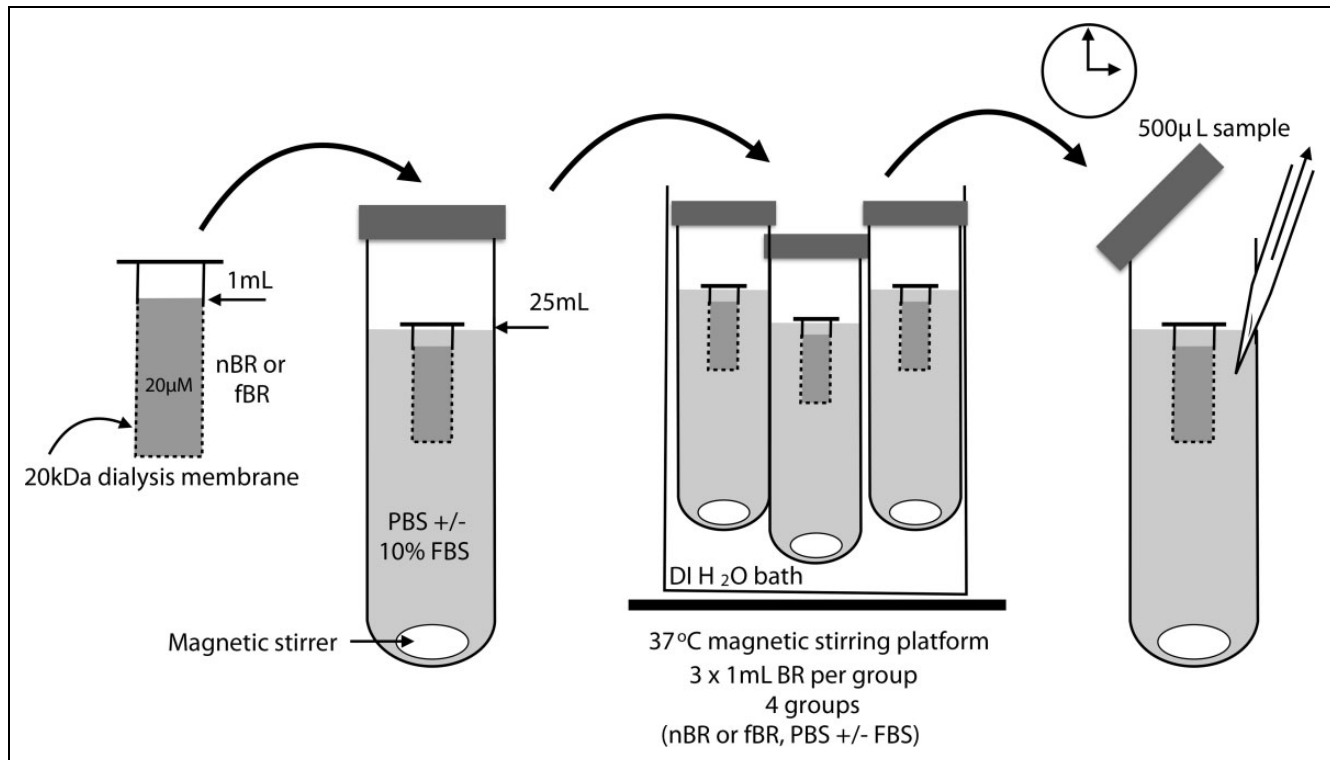


Fig. 3. Procedure for testing the release characteristics of nanoparticle bilirubin (nBR) and free bilirubin (fBR) in solutions with or without protein. Aliquots of 1 mL of $\sim 20 \mu\text{M}$ fBR or nBR were suspended within a 20 kD Spectra/Por dialysis tube, in 25 mL of either phosphate-buffered saline (PBS) or PBS containing 10% fetal bovine serum (FBS) and 1% penicillin/streptomycin. Samples were incubated at 37°C , continuously agitated with magnetic stirrer bars and protected from light. A total of $500 \mu\text{L}$ of dialysate were taken at predetermined time points for a period of 3 d, and the samples of dialysate were frozen at -20°C . Spectrophotometric analysis was performed at 460 nm to determine the bilirubin concentration in each sample using a standard curve of known bilirubin concentrations.

Pluronic–chitosan NPs in DI water under constant stirring. After 1 h of equilibration, the sample was put under low vacuum to remove chloroform slowly over 6 to 8 h. Then the sample was transferred into a round flask to remove any remaining chloroform by rotary evaporation. The sample was then filtered through a $0.45 \mu\text{m}$ filter at room temperature and lyophilized for 24 h to obtain dry nBR (Fig. 2C) that were either used immediately or stored at -20°C for future use.

Spectrophotometric Analysis of Bilirubin Content Within Nanoparticles

Bilirubin is a bile pigment that exhibits strong autofluorescence, with maximum spectral absorption at a wavelength of 440 nm when in aqueous solution and 480 nm when bound to bovine serum albumin (BSA).^{17,18} To determine the dose of nBR required for the ensuing experiments, 1 mg/mL nBR in phosphate-buffered solution (PBS) was compared to a standard curve of known bilirubin concentrations via spectrophotometric analysis at the wavelength of 440 nm . The 1 mg/mL nBR in PBS was found to have a bilirubin concentration of $4.8 \mu\text{M}$. Further calculations of the dose of nBR or eNP were performed based on weight, with the assumption

that 1 mg of nBR and 1 mg of eNP contained equivalent numbers of NPs.

In Vitro Release Studies

Aliquots of 1 mL of $\sim 20 \mu\text{M}$ fBR or nBR were suspended within a 20 kD Spectra/Por (Spectrum Laboratories, Irving, TX, USA) dialysis tube, in 25 mL of either PBS or PBS containing 10% FBS and 1% penicillin/streptomycin. The pore size of the dialysis membrane was selected based on the relative sizes of unconjugated bilirubin molecules (0.585 kDa), BSA (66.5 kDa), and radius of the NP ($\sim 20 \text{ nm}$ at 37°C). Pores of the 20 kDa dialysis tube would allow diffusion of spherical molecules with a radius of 1.78 nm or smaller.¹⁹ Thus, fBR would be able to pass through the pores, while NPs and albumin would not. Three samples were tested for each of the 4 groups. Samples were incubated at 37°C , continuously agitated with magnetic stirrer bars and protected from light (Fig. 3). A total of $500 \mu\text{L}$ of dialysate was taken at predetermined time points for a period of 3 d and, the dialysate was replaced with an equal volume of the base solution each time. The samples of dialysate were frozen at -20°C . After all samples were collected, spectrophotometric analysis was performed at 460 nm to determine the bilirubin concentration in each sample using a standard

curve of known bilirubin concentrations. Results were expressed as percentage release compared to initial concentration of bilirubin within the dialysis tube.

Cellular Uptake and Intracellular Distribution of nBR in INS-R3 Cells

Murine INS-R3 cells, an insulinoma cell line, were used as a model of pancreatic β cells. Following cell culture to confluence, cells were seeded into 35 mm petri dishes at 1.5×10^5 cells/dish with 1 mL RPMI cell culture medium. Each petri dish also contained two 12 mm type I collagen-coated glass cover slips, to allow cell adherence. Glass coverslips were dipped in type I collagen solution (1 mg/mL) in PBS (1 \times by default) for 1 min and then dried in cell culture hood for 15 min in air at room temperature before experiments.

Following overnight incubation at 37 °C, cells were further treated with RPMI cell culture media containing 0, 5, 10, or 20 μ M nBR, fBR, or empty NP (eNP), as well as 75 nM LysoTracker Red DND-99 (Life Technologies, Grand Island, NY, USA) to fluorescently label acidic organelles (lysosomes). After 1 h incubation at 37 °C, the cells were washed twice with 37 °C PBS and fixed with 4% paraformaldehyde at 37 °C for 10 min. The fixed cells were then incubated with Hoechst 33342 (5 μ M in PBS) for 10 min at 37 °C and washed twice with 37 °C PBS to stain their nuclei. Finally, the coverslips with attached cells were mounted onto glass slides with Vectashield antifade mounting medium (Vector Laboratories, Burlingame, CA, USA) for further examination. The intracellular bilirubin uptake by INS-R3 cells and distribution of bilirubin within the cells were studied qualitatively using Zeiss Apotome (Oberkochen, Germany) confocal-like structured illumination microscopy (SIM). Bilirubin demonstrates fluorescence emission at a wavelength of 534 nm when associated with plasma membranes.²⁰ Thus, intracellular bilirubin can be detected using a green excitation fluorescence filter, which covers a wavelength of 510 to 560 nm.

Effects of nBR on Viability of INS-R3 Cells Exposed to Hypoxic Stress

Further, INS-R3 cells were then cultured until a monolayer had formed were then seeded into 24-well cell culture plates at a density of 5×10^4 cells per well in 1 mL cell culture media per well. Media was treated with nBR, fBR, or eNP at concentrations of 0 to 20 μ M (2 wells per treatment dose). Cells were acclimatized for 4 h under standard incubator conditions (21% O₂ at 37 °C), then exposed to 8 h hypoxia (1% O₂), followed by 12 h recovery (standard conditions). The 3-[4,5-dimethylthiazol-2-yl]-2,5-diphenyltetrazolium bromide (MTT) viability assays were performed as follows: 50 mg MTT was dissolved in RPMI cell culture solution (without phenol red) to create MTT stock solution. MTT stock solution of 100 μ L was added to each well, and samples were incubated for 1 h at 37 °C. Media was aspirated from

the wells, cells were rinsed in 1 mL PBS (1 \times) and, 0.5 mL dimethyl sulfoxide (DMSO) was added to each well. Aliquots of 200 μ L of the reaction product were transferred to a 96-well plate (2 samples per well of the 24-well plate), and absorbance was measured via spectrophotometry at a wavelength of 562 nm. Cell viability was expressed as percentage absorbance of control (untreated) cells.

Effects of nBR on Viability of Murine Islets Exposed to Hypoxic Stress

Experiments were approved by the Institutional Animal Care and Use Committee at The Ohio State University (protocol # 2012 A0000121). To assess the effects of nBR, fBR, and eNP treatment on viability of murine pancreatic islet cells in vitro, mouse pancreatic islets were isolated from female C57BL/6 donors (Harlan laboratories, Indianapolis, IN, USA) and maintained in culture using the techniques described by Zmuda et al.²¹ Following 24 h incubation at 37 °C, islets were transferred to 35 mm petri dishes at a density of ~ 60 islets per dish and suspended in 1 mL media containing either nBR, fBR, or eNP at concentrations of 0, 5, 10, or 20 μ M. Cells were incubated under standard conditions (37 °C, 21% O₂) for 4 h, then exposed to 24 h of hypoxia (1% O₂ at 37 °C), followed by 12 h of recovery under standard culture conditions. Media was changed for fresh media containing equivalent drug concentrations prior to recovery. The duration of hypoxia was based on previous work in our laboratory, with the goal of achieving 30% to 40% cell death in order to demonstrate both potential detrimental and therapeutic effects of NP administration.⁵ Islets were hand-picked and transferred to new 35 mm petri dishes containing propidium iodide (PI) and 5 μ M Hoescht 33342 in PBS. Cells were imaged using 4',6-diamidino-2-phenylindole (DAPI) (blue) and Texas Red (red) channels via epifluorescent microscopy. Images were analyzed using NIH Image J software; and the percentage of PI positive cells, indicating percentage cell death present in each islet, was calculated using a custom islet macro as previously described.²²

Islet function testing using glucose-stimulated insulin secretion. To assess islet function following treatment with various concentrations of nBR, fBR, or eNP, further mouse pancreatic islets were isolated and cultured overnight in RPMI cell culture media with 10% penicillin/streptomycin and 1% BSA, containing 5 or 10 μ M of nBR, fBR, or eNP, or no treatment (control). Experiments were repeated 3 times. Following overnight incubation, islets of different mice were mixed and incubated for 2 h in zero glucose media (Krebs-Ringers bicarbonate buffer solution containing 0.1% BSA). Islets were then hand-picked and transferred to 35 mm petri dishes containing 1 mL each of either low-glucose (2.8 mM) or high-glucose (28 mM) media (Krebs-Ringers bicarbonate buffer, 1% BSA, containing D-glucose) and incubated at 37 °C for 1 h with gentle agitation. Insulin concentrations in the media were measured using commercially available assays

Table 1. EE and LC of Bilirubin Together with Diameter of the Resultant NP-Encapsulated Bilirubin (nBR), Determined by DLS: All Data are Presented as Mean \pm Standard Deviation.

NP type	Bilirubin: NP Ratio (w: w)	EE (%)	LC (%)	NP=Diameter, nm at 22 °C	NP Diameter, nm at 37 °C	NP Zeta Potential, mV at 22 °C	NP Zeta Potential, mV at 37 °C
nBR	1: 20	10.1 \pm 0.2	0.6 \pm 0.1	355.0 \pm 9.3	27.1 \pm 1.4	4.4 \pm 0.4	19.1 \pm 4.9
eNP	NA	NA	NA	293.7 \pm 47.7	19.0 \pm 1.9	9.3 \pm 0.6	20.7 \pm 0.7

Abbreviations: DLS, dynamic light scattering; eNP, empty nanoparticle; EE, encapsulation efficiency; LC, loading content; nBR, nanoparticle bilirubin; NA, not applicable; NP, nanoparticle.

(Mercodia Mouse Insulin ELISA; Uppsala, Sweden). To account for differences in islet size and therefore absolute insulin secretion between groups, insulin secretion was normalized according to DNA content. The stimulation index (SI) was calculated as the normalized insulin concentration in high-glucose media divided by the normalized insulin concentration in low-glucose media, for each group.

Statistical Analyses

Statistical analyses for release data were performed using MedCalc for Windows, version 12.5 (MedCalc Software, Ostend, Belgium). Area under the curve (AUC) was analyzed using the Kruskal-Wallis nonparametric test with Conover posttests. Following outlier detection using Grubbs double-sided and Tukey tests, the analysis was rerun with outliers excluded, and the results were unchanged. Cell viability data were analyzed using IBM SPSS Statistics for Mac, Version 21.0 (IBM Corp, Armonk, NY, USA). Shapiro-Wilk and Levene tests were used to test data for normal distribution and homoscedasticity, respectively. For INS-R3 cell viability data, 2-factor, univariate analysis of variance (ANOVA) was performed, and Tukey honest significant difference post hoc tests were used to compare effects between groups. For murine islet cell viability data, the main effects of “treatment group” and “concentration” on the dependent variable “percentage cell death” were evaluated with the linear mixed procedure. When a significant main effect was identified, a multiple comparison test (Sidak) was performed. Islet function data (SI based on normalized insulin secretion for each group) were analyzed using 2-factor, univariate ANOVA. SI data were log transformed prior to analysis to better fit the assumptions of the statistical model. Statistical significance was set at $P \leq 0.05$.

Results

Physicochemical Characterization of Nanoparticles

The morphology, size, and ζ potential of Pluronic F127–chitosan NPs were determined using the techniques reported by Rao et al.¹⁶ Briefly, transmission electron microscopy and a carbon film-coated copper transmission electron microscopy grid were used to visualize NP size, whereas surface ζ potential of nanomaterials (i.e., NP and nBR) were assessed using

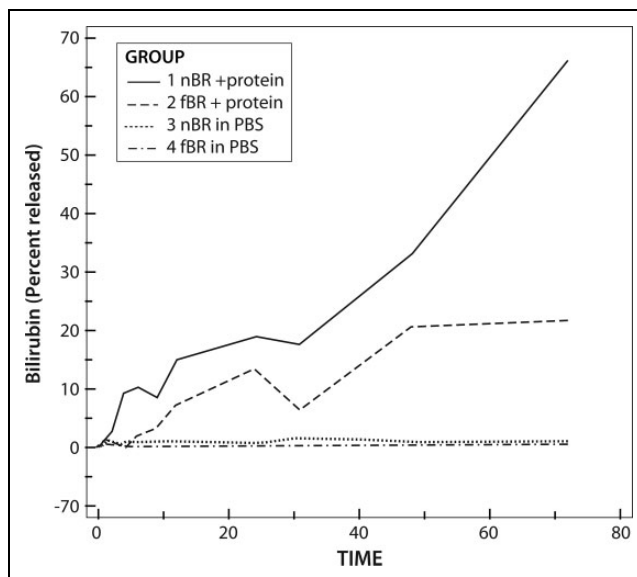


Fig. 4. Release of bilirubin, expressed as percentage of original bilirubin concentration, through a 20 kDa dialysis membrane, suspended in dialysate with or without protein. Group 1: nanoparticle bilirubin (nBR) in phosphate-buffered solution (PBS) + 10% albumin; Group 2: free bilirubin (fBR) in PBS + 10% albumin; Group 3: nBR in PBS; Group 4: fBR in PBS. Area under the curve for bilirubin release in each of the 4 groups was significantly different ($P = 0.0156$). Release was significantly greater for nBR than for fBR and in solutions containing protein compared to PBS alone ($P < 0.001$). For nBR in PBS + 10% FBS, there was an initial burst of release over approximately 8 h, followed by a more steady release up to 48 h.

a Brookhaven 90Plus/BI-MAS (Holtsville, NY, USA) dynamic light scattering (DLS) instrument. Results are presented in Table 1.

Bilirubin Release Characteristics

AUC for bilirubin release in each of the 4 groups was significantly different ($P = 0.0156$). Release was significantly greater for nBR than for fBR and in solutions containing protein compared to PBS alone ($P < 0.001$). For nBR in PBS + 10% FBS, there was an initial burst of release over approximately 8 h, followed by a more steady release up to 48 h. The initial burst release was not as marked for the fBR group, but maximal bilirubin release occurred over the first 48 h, followed by a plateau of the release curve (Fig. 4).

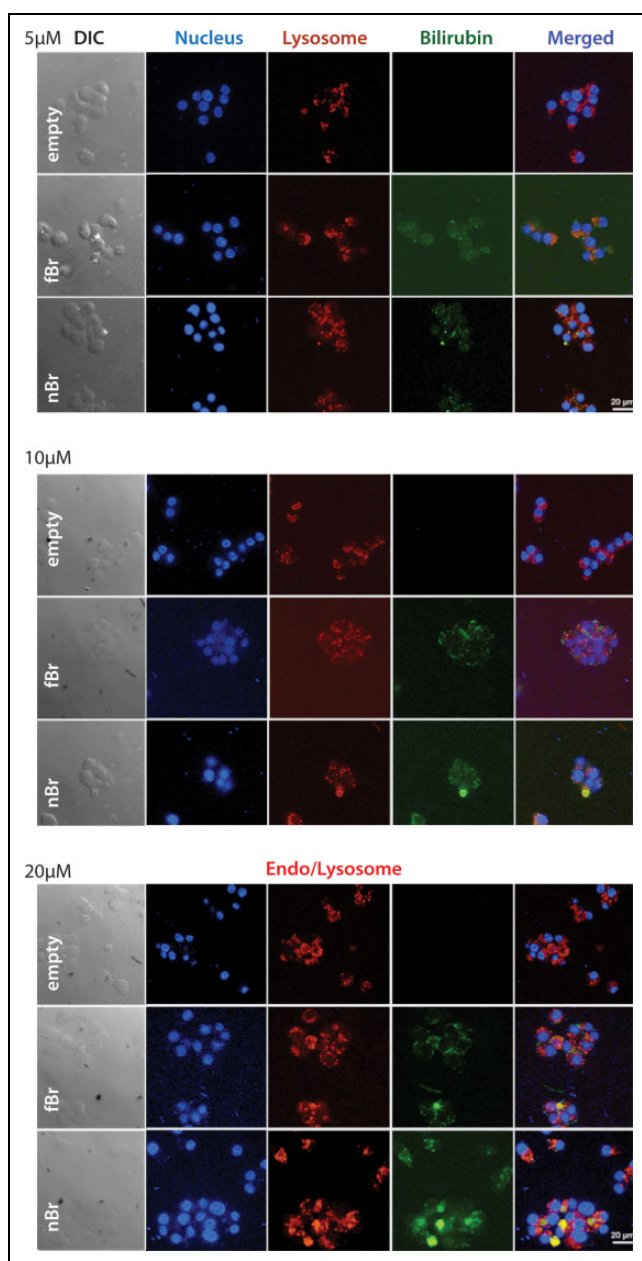


Fig. 5. Uptake of nanoparticle bilirubin (nBR; bottom row of each image), free bilirubin (fBR; middle row), and empty nanoparticles (eNP; top row), at concentrations of 5 μ M, 10 μ M, and 20 μ M, by INS-R3 cells in culture. Murine INS-R3 cells in culture were seeded into petri dishes containing RPMI cell culture medium and type I collagen-coated glass cover slips, to allow cell adherence. Cells were further treated with RPMI cell culture media containing 0, 5, 10, or 20 μ M nBR, fBR, or eNP, as well as 75 nM LysoTracker Red DND-99 to fluorescently label lysosomes. Cells were fixed and then incubated with Hoechst 33342 nuclear stain. Intracellular bilirubin uptake and distribution of bilirubin within the cells were studied qualitatively using Zeiss Apotome (confocal-like) structured illumination microscopy. INS-R3 cells showed increased uptake of nBR compared to fBR, which was dose-dependent. In cells treated with 10 to 20 μ M nBR, colocalization of nanoparticles within endo-lysosomes was demonstrated as overlay of the LysoTracker Red and bilirubin (green) fluorescence, resulting in a cumulative yellow color.

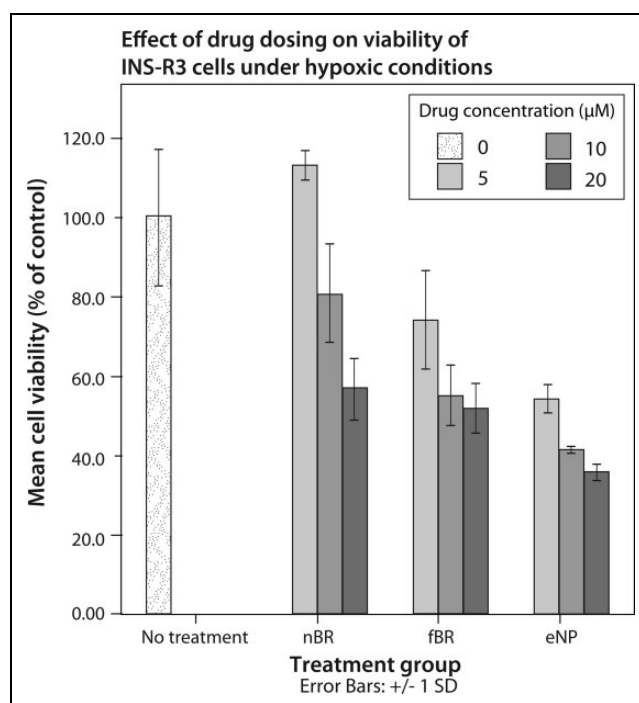


Fig. 6. Mean viability \pm standard deviation, expressed as percentage of viability of untreated cells, of INS-R3 cells treated with 0 to 20 μ M nanoparticle bilirubin (nBR), free bilirubin (fBR), or empty nanoparticle (eNP) and exposed to 8 h hypoxia. INS-R3 cells were cultured and then treated with media containing nBR, fBR, or eNP at concentrations of 0 to 20 μ M. Cells were exposed to 8 h hypoxia (1% O_2), followed by 12 h recovery (standard conditions). The 3-[4,5-dimethylthiazol-2-yl]-2,5-diphenyltetrazolium bromide (MTT) viability assays were performed, and absorbance was measured via spectrophotometry at a wavelength of 562 nm. Cell viability was expressed as percentage absorbance of control (untreated) cells. Treatment group and concentration had significant effects on percentage cell death ($P < 0.001$), and there was a significant interaction between the 2 factors ($P = 0.014$). The highest viability was seen in cells treated with 5 μ M nBR ($113.2\% \pm 3.9\%$ of control).

Cellular Uptake of Bilirubin in INS-R3 Cells

INS-R3 cells showed increased uptake of nBR compared to fBR, which was dose-dependent. In cells treated with 10 to 20 μ M nBR, colocalization of NPs within acidic organelles (endo-lysosomes) was demonstrated as overlay of the LysoTracker Red and bilirubin (green) fluorescence, resulting in a cumulative yellow color (Fig. 5).^{23,24}

Effects of nBR on INS-R3 Cells under Hypoxic Conditions

In INS-R3 cells exposed to hypoxic stress, treatment group and concentration had significant effects on percentage cell death ($P < 0.001$), and there was a significant interaction between these 2 factors ($P = 0.014$). Cell viability data are expressed as percentage viability compared to untreated cells \pm standard deviation in Fig. 6. The highest viability was seen in cells treated with 5 μ M

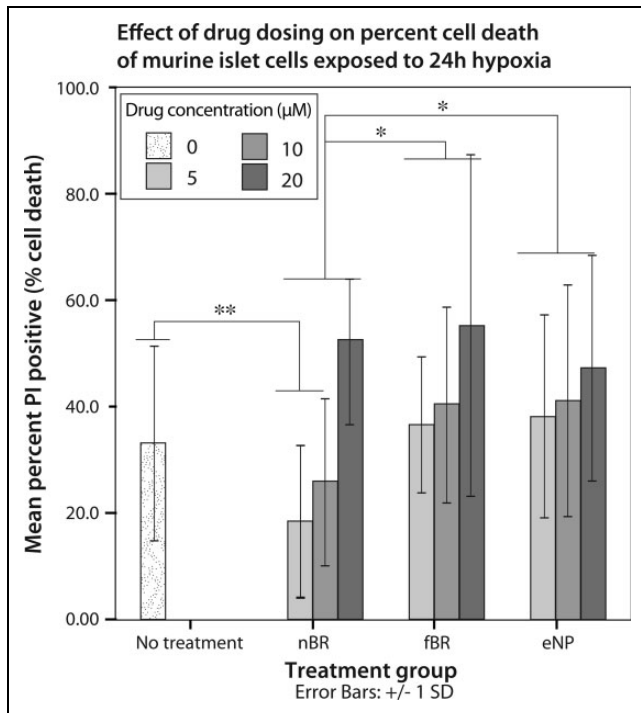


Fig. 7. Mean cell death \pm standard deviation, expressed as percentage PI positive cells, of murine islets treated with 0 to 20 μ M nanoparticle bilirubin (nBR), free bilirubin (fBR), or empty nanoparticle (eNP) and exposed to 24 h hypoxia. Mouse pancreatic islets were isolated from female C57BL/6 donors and maintained in culture. Following 24 h incubation at 37 °C, islets were suspended in 1 mL media containing either nBR, fBR, or eNP at concentrations of 0, 5, 10, or 20 μ M. Cells were incubated under standard conditions (37 °C, 21% O₂) for 4 h and then exposed to 24 h of hypoxia (1% O₂ at 37 °C) followed by 12 h of recovery under standard culture conditions. Islets were stained with propidium iodide and Hoescht 33342 in phosphate-buffered solution (PBS). Cells were imaged using DAPI (blue) and Texas Red (red) channels via epifluorescent microscopy. Percentage of PI positive cells, indicating percentage cell death present in each islet, was calculated. Treatment group ($P = 0.05$) and concentration ($P < 0.001$) had significant effects on percentage cell death. Interaction between the 2 factors was not significant ($P = 0.062$). Overall, islets treated with nBR ($24.7\% \pm 17.5\%$) had significantly decreased percentage cell death compared to those treated with fBR ($43.9\% \pm 23.4\%$; $P = 0.047^*$) or eNP ($42.1\% \pm 21.0\%$; $P = 0.005^*$). Islets treated with 5 μ M nBR ($18.5\% \pm 14.1\%$) or 10 μ M nBR ($25.7\% \pm 15.7\%$) had significantly decreased cell death compared to untreated islets ($33.5\% \pm 17.5\%$; $P = 0.019^{**}$). Dose-dependent cytotoxicity was seen in all groups, with 20 μ M fBR, nBR, and eNP having significantly higher cell death in every group when compared to doses of 5 to 10 μ M ($P \leq 0.007$).

nBR, while treatment with empty NPs appeared to decrease viability of INS-R3 cells.

Protective Effects of nBR on Murine Islets under Hypoxic Conditions

In murine islets exposed to hypoxic stress, treatment group ($P = 0.05$) and concentration ($P < 0.001$) had significant

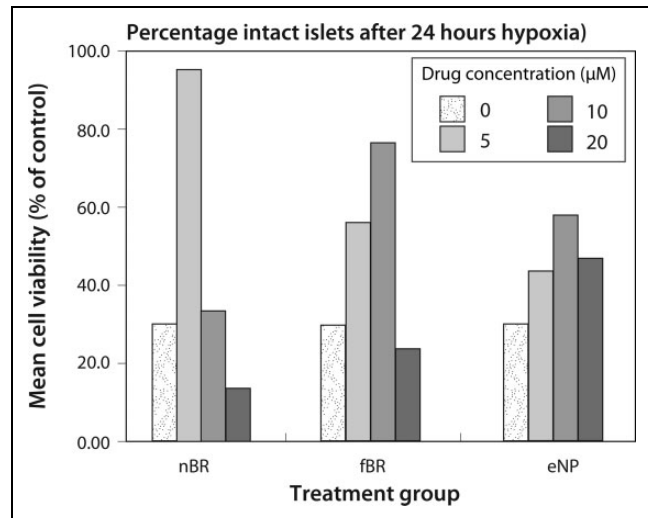


Fig. 8. Islet survival, expressed as percentage of initial number of islets, after treatment with 0 to 20 μ M nanoparticle bilirubin (nBR), free bilirubin (fBR), or empty nanoparticle (eNP) and exposure to 24 h hypoxia. At 12 h after a 24-h period of hypoxia, the number of remaining intact islets in each group was divided by the initial islet count (60 islets per well) to determine the percentage of islets persisting in culture. Islets treated with 5 μ M nBR (95.0% intact) and 10 μ M fBR (76.7% intact) had a higher percentage of intact islets when compared to control (30% intact).

effects on percentage cell death. Interaction between these 2 factors was not significant ($P = 0.062$). Data are expressed as mean cell death ($\%$) \pm standard deviation. Overall, islets treated with nBR ($24.7\% \pm 17.5\%$) had significantly decreased percentage cell death compared to those treated with fBR ($43.9\% \pm 23.4\%$; $P = 0.047$) or eNP ($42.1\% \pm 21.0\%$; $P = 0.005$; Fig. 7). Islets treated with 5 μ M nBR ($18.5\% \pm 14.1\%$) or 10 μ M nBR ($25.7\% \pm 15.7\%$) had significantly decreased cell death compared to untreated islets ($33.5\% \pm 17.5\%$; $P = 0.019^{**}$). Dose-dependent cytotoxicity was seen in all groups, with 20 μ M fBR, nBR, and eNP having significantly higher cell death in every group when compared to doses of 5 to 10 μ M ($P \leq 0.007$).

At 12 h after a 24-h period of hypoxia, the number of remaining intact islets in each group was divided by the initial islet count (60 islets per well) to determine the percentage of islets persisting in culture. Islets treated with 5 μ M nBR (95.0% intact) and 10 μ M fBR (76.7% intact) had a higher percentage of intact islets when compared to control (30% intact; Fig. 8).

When images of stained islets were analyzed qualitatively (Fig. 9), central necrosis of islets was seen in untreated groups, as well as those treated with fBR at concentrations of 10 to 20 μ M. Central apoptosis and necrosis being is particularly pronounced in central areas of large islets due to the higher nutrient and oxygen diffusion distance to the center of these cell aggregates.²⁵

Islet function measured by glucose-stimulated insulin secretion. There was a significant effect of treatment group on SI

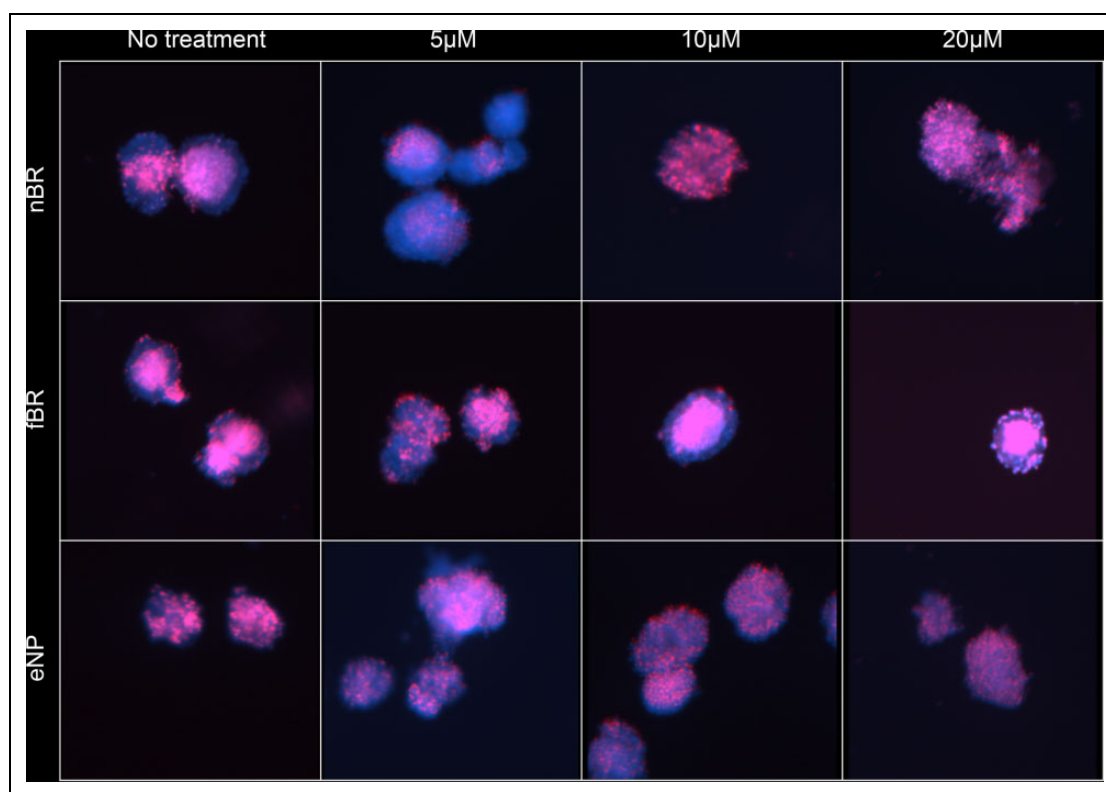


Fig. 9. Hoescht (nuclear, blue) and PI (cell death, red) staining of murine islets treated with 0 to 20 μM nanoparticle bilirubin (nBR), free bilirubin (fBR), or empty nanoparticle (eNP) and exposed to 24 h hypoxia. Images were taken using epifluorescent microscopy at $4\times$ magnification. Qualitative analysis of stained islets revealed central necrosis of islets in untreated groups, as well as those treated with fBR at concentrations of 10 to 20 μM . Apoptosis and necrosis are particularly pronounced in central areas of large islets due to the higher diffusion distance to the center of these cell aggregates.

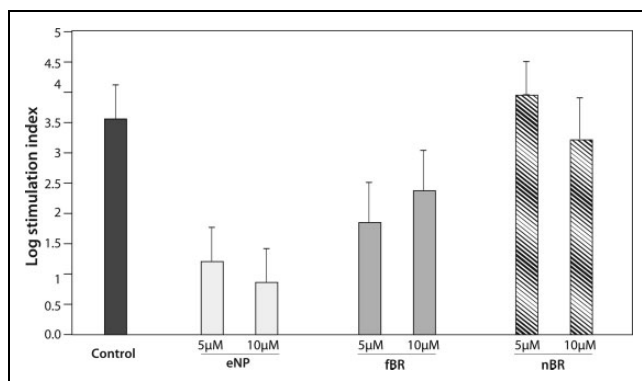


Fig. 10. Assessment of islet function in murine islets. Glucose stimulation index (SI) was calculated as the ratio of normalized insulin secretion in high: low glucose media for untreated islets and for those treated with 5 to 10 μM empty pluronic F127–chitosan nanoparticles (eNP), free bilirubin (fBR), or nanoencapsulated bilirubin (eNP). Increasing SI indicates improved islet viability. Data were log transformed to better fit the assumptions of the statistical model and are presented as mean \pm standard error. There was a significant effect of treatment group on log SI ($P = 0.014$), with the highest SI seen in islets treated with 5 μM nanoencapsulated bilirubin (nBR). Empty nanoparticles (ENP) appeared to have a negative effect on islet function, which increased with increasing dosages from 5 to 10 μM .

($P = 0.0137$), with the highest SI noted in islets treated with 5 μM nBR. Islets treated with fBR and particularly those treated with empty NPs had lower SI than control, suggesting that both fBR and empty NPs had a negative effect on islet function (Fig. 10).

Discussion

Although several researchers have demonstrated the protective effects of bilirubin in research models, our study is the first to use NP drug delivery to take a step toward a more bioavailable and therefore clinically applicable drug formulation. Drug release studies in our novel in vitro model showed some surprising results. The release kinetics of entrapped drug from polymeric micelles into the dialysis chamber is affected by diffusion of drug and polymer degradation—Pluronic F127 polymers undergo degradation by hydrolysis in PBS solution.^{26,27} Using the dynamic dialysis method as in this study, the apparent release rate is the net result of drug transport across 2 barriers in series: release from the NPs into the dialysis chamber followed by diffusion across the dialysis membrane.²⁸ Previous studies of drug release from Pluronic F127–chitosan NPs suspended in PBS report an initial release “burst” over 8 h, followed by sustained drug release over the ensuing 48 h, with plateau of the

release curve after 48 h.^{24,29} A key difference in our study is that it is the first to use protein in the dialysate solution in an attempt to better simulate *in vivo* release kinetics—something that we considered important in evaluating the release of bilirubin, which is a highly protein-bound substance. Using this model, we found that significantly greater bilirubin release occurred in solutions containing albumin (FBS), compared to PBS alone, which is likely related to the high affinity of bilirubin for albumin in aqueous solution. Unconjugated bilirubin has poor solubility at pH 7.4 (~70nM), but this is improved in plasma, where 99% of bilirubin (IX α) is bound to albumin in human adults.⁹ Human serum albumin (HSA) has 1 high-affinity binding site—an L-shaped “pocket” in subdomain IB—and 1 or 2 secondary binding sites with much lower affinity for bilirubin.³⁰ BSA has a molecular weight almost identical to HSA (66.5 kDa) and the stoichiometry of bilirubin binding to BSA is thought to be comparable to HSA, with 1 high-affinity and 2 low-affinity binding sites.¹⁸ Bilirubin, complexed to albumin, may have been more stable in solution and diffused more readily across the dialysis membrane than in solutions of PBS alone, where the hydrophobic bilirubin may have precipitated.

Another unexpected finding in the release study was the relatively slower diffusion of fBR across the dialysis membrane compared to nanoencapsulated bilirubin. Since nBR first had to dissociate from NP, then diffuse across the membrane, slower drug release from the nBR group would have been expected. However, previous studies citing sustained release of drug from NP did not report parallel release data for diffusion of free drug across the same membrane, so we have no basis for comparison.

Although dynamic dialysis is the standard method for evaluation of drug release from NP formulations, a recent study²⁸ questioned the validity of this method. These authors proposed that the dual barrier (release from NP, followed by diffusion across a membrane) complicates data interpretation and may lead to incorrect assumptions about sustained release from NP carriers, since reversible binding of drug to NP within the dialysis membrane determines the drug concentration available for diffusion. They recommended validation of drug release kinetics at varying NP concentrations and the determination of membrane-binding coefficients along with appropriate mechanism-based mathematical modeling to ensure the reliability and proper interpretation of the data.²⁸ Additional investigation of drug release kinetics, using ultracentrifugation and ultrafiltration to separate NP from free drug at each time point in the study, as well as continuing the release study over a longer time period would add further information to the release kinetics data generated in the current study.

Nanoparticle delivery of bilirubin achieved a protective effect in isolated murine islets, following hypoxic stress. The mechanism of the improved effects of nBR when compared to fBR is likely the improved, selective uptake of nBR by pancreatic islet cells. Cellular uptake is influenced by NP

size and ζ potential. Smaller NPs have a larger surface area, leading to greater cellular uptake and faster release of drug. The nBR particles used in this study, with a diameter 27.1 nm at 37 °C, were within the ideal range for uptake via endocytosis of 10 to 30 nm.³¹ In addition, the positive surface charge of nBR at 37 °C (19.1 ± 4.1 mV) likely facilitated its uptake by mammalian cells, whose plasma membrane is usually negatively charged.¹⁶

Pancreatic β cells are metabolically active, especially under conditions of increased glucose concentration. The stimulation of insulin release by glucose is accompanied by an enhanced uptake of macromolecules, via a specific exocytosis-endocytosis coupling mechanism.³² However, the cellular entry of macromolecules like bilirubin, via simple diffusion, is impaired by the poor permeability and selectivity of cell membranes and by degradation within lysosomes following internalization by endocytosis. Polymeric NPs are capable of escaping degradation within the endo-lysosomal compartment, resulting in more efficient intracellular delivery.³³

LysoTracker Red is a fluorescent marker for secondary endosomes and lysosomes, which is colorless at physiologic pH, but has red fluorescence at the acidic pH of 4 to 5 of endosomal compartments. In the current study, when nBR (green fluorescence) was colocalized within the endo-lysosomal compartment with LysoTracker Red, yellow fluorescence resulted. However, at 1 h postincubation, some nBR was also localized in the cytoplasmic compartment, as seen from the appearance of green fluorescence of NPs (Fig. 5). This is consistent with the findings of previous studies of Pluronic F127–chitosan NP, and it can be inferred that NPs were probably escaping rapidly from the endo-lysosomal compartments into the cytoplasmic compartment following their uptake.^{12,33} These observations indicate that endocytosis via the endosome/lysosome system is an important mechanism for cellular uptake of the Pluronic F127–chitosan nBR.

This study showed a trend toward a protective effect of 5 μ M nBR in insulinoma cell line (INS-R3) cells exposed to hypoxic stress (Fig. 6), but protective effects were less apparent than those seen in intact murine islets (Figs. 8 and 9). Since the MTT assay provides cell viability data relative to control cells, rather than as an absolute value, it is not possible to compare percentage cell death overall between INS-R3 and murine islet cells following hypoxia. However, it is likely that the cancer cell line was less susceptible to the detrimental effects of hypoxia than pancreatic islets, which may have resulted in attenuation of the protective effects of NP. In a previous study characterizing cell death in murine islets and MIN6 insulinoma cell line cells exposed to transplant stressors *in vitro*, murine islets were found to exhibit marked plasticity in cell death modes, in contrast to MIN6 cells, which died almost exclusively via classical apoptosis.³⁴ These observations suggest that insulinoma cell lines may not be an appropriate or representative model for murine pancreatic islets in future experiments. Another

explanation for the modest protective effects of nBR in INS-R3 cells is that neoplastic cells tend to accumulate larger numbers of NP through endocytosis, due to their increased metabolic activity. This may have resulted in a relative overdose of NP polymers, overwhelming any protective effects of nBR.

Doses of 5 to 10 μM nBR were protective of murine pancreatic islets following hypoxic stress, in agreement with previous studies, which reported therapeutic doses of fBR of 8.5 to 10 μM .^{7,12} In general, the dosing efficiency of nano-encapsulated drug is expected to be greater than free drug, due to sustained drug release combined with rapid, preferential uptake by metabolically active cells.³⁵ Targeted drug delivery to islets, using an islet-specific ligand, such as an "islet-homing peptide,"²⁴ may further increase the efficiency of nBR and reduce the therapeutic dose. Interestingly, while nano-encapsulation of bilirubin appeared to improve biological effect and drug delivery, the therapeutic range of this novel formulation remains narrow, as with fBR. Fortunately, if the drug is being administered *ex vivo* in islet media prior to transplantation, drug concentrations will be easier to predict when compared to systemically administered drugs.

We noted that treatment of islets with nBR prevented central necrosis of islets when PI images were assessed qualitatively (Fig. 9). Untreated islets and those treated with $>5\mu\text{M}$ fBR exhibited characteristic central necrosis, whereas islets treated with 5 μM nBR did not. Giuliani et al.²⁵ investigated the relative effects of hypoxia (1% oxygen for 24 h) and nutrient deprivation on pancreatic islets and MIN6 insulinoma cells and concluded that the gradual transition from an apoptotic to a necrotic morphology in the central cells of hypoxic pancreatic islets is the result of the combined effects of hypoxia and nutrient or serum deprivation, most likely due to impaired diffusion. The mechanism by which nBR protects against central necrosis may be improved uptake of nBR by central islet cells, compared to fBR, since uptake of nBR appears to be via active transport, rather than simple diffusion as for fBR. Previous work in our laboratory investigating the protective effects of fBR on isolated murine islets exposed cells to 3 h hypoxia found significant improvements in cell survival. However, exposure to 24 h hypoxia may have overwhelmed the protective effects of fBR and highlights the improved effectiveness of NP drug encapsulation. This effect may have variable clinical importance in difference species. For example, in canine islet transplantation, since both murine and canine islets are composed primarily of β cells clustered in a central core, surrounded by smaller numbers of α cells, δ cells, PP cells, and ϵ cells in the periphery. This is in contrast to human islets, which have fewer β -cells, randomly distributed throughout the islet.³⁶ In a similar manner, differences in islet anatomy and physiology between species may cause variations in sensitivity of the islets to hypoxic injury and future studies will be required to investigate the dose effects of nBR therapy in canine and human islets.

Islets treated with 5 to 10 μM nBR and 10 μM fBR demonstrated improved insulin secretion in response to glucose compared to untreated islets, and SI was highest in the 5 μM nBR group. These data on islet function are aligned with the viability data for the various treatment groups and support that at a concentration of 5 μM , nBR appeared to improve both islet viability and function. Interestingly, our model showed evidence that eNP caused a dose-dependent decrease in islet function. There was substantial variability in normalized insulin secretion data for islets treated with eNP (Fig. 10), with higher insulin concentrations in media under "basal" glucose conditions, and lower insulin concentrations in "high"-glucose media. One possible explanation is that islets underwent necrosis or apoptosis when treated with eNP (as was observed in islet hypoxia experiments) and released cytosolic insulin into media prior to stimulation with glucose.

SI, the ratio of insulin level in culture media containing high:low glucose concentrations, is an accepted measure of islet function and is the most frequently used test in clinical and experimental studies.^{37,38} Typically, islets are cultured in a "low"-glucose concentration, near 3 mM, to measure the amount of insulin secreted into the media under "basal" conditions. Stimulated insulin release is measured by exposing islets to a higher glucose concentration of 11.1 mM (half-maximal) to 28 mM (maximal—used in this study).³⁷ Insulin release from islets is biphasic, with an initial spike in insulin release after 5 to 6 min (first phase) followed by a decline to a prolonged second phase plateau of insulin release that begins about 60 min after stimulation and persists for the duration of the stimulus.^{37,39} SI of healthy islets varies from 2 to 20, depending on strain, age, and bodyweight of donor animals, and a cutoff value of SI >3 has been shown to be predictive of viable islets when high-glucose concentrations of 16.5 to 22 mM are used.^{37,38} In the current study, insulin secretion data were normalized based on islet DNA content, the SI cannot be directly compared to previous reports. In addition, concentrations of glucose in "high" glucose media often differ between studies, hindering comparison between institutions.³⁸ The release of insulin from islets is a complex process, modulated not only by glucose but also by nonglucose nutrients, hormones, and neural inputs.³⁹ Other studies have investigated alternative methods of testing islet viability, including adenosine diphosphate (ADP)/adenosine triphosphate (ATP) ratio, ATP/DNA ratio, or insulin/DNA ratio, since intracellular DNA remains relatively stable within dead cells, allowing their inclusion in the overall assessment of viability.^{38,40,41} However, there is no consensus on a gold standard test for predicting islet viability and success of transplant *in vivo*, and SI remains the clinical standard in human islet transplant programs.

Interestingly, eNPs were found to be toxic to both INS-R3 cells and murine islets, following hypoxic stress. Treatment of murine islets with eNP at 5 to 10 μM resulted in a higher rate of cell death (measured via PI staining) and a lower number of intact islets than treatment with nBR at the same

doses. In addition, islets treated with eNP had the lowest SI overall, indicating impaired islet function. Murine islets and INS-R3 cells in this experiment were treated with 1 to 4 mg/mL nBR or eNP, in order to achieve bilirubin concentrations of 5 to 20 μ M. Given the low loading content of the nBR (0.6% by weight of each NP), toxicity may have resulted from the relatively higher dose of NP needed to achieve therapeutic doses of bilirubin. Having seen the improved drug release and uptake in the current study, it is interesting to speculate whether even lower doses of nBR (<5 μ M) would retain the positive biological effects demonstrated herein and would further minimize any cytotoxicity resulting from the NP formulation.

Some previous studies of the effects of Pluronic F127–chitosan NP on both cancerous and noncancerous cultured cell lines *in vitro* have found low toxicity (>95% viability) at doses of 1 to 10 mg/mL.^{12,29} In contrast, a study investigating poly(lactic-co-glycolic acid) and poly(ethylene glycol) or PLGA-PEG NP for delivery of an immunosuppressive drug to murine islet capillary endothelial cells *in vitro* found a dose-dependent pro-inflammatory effect of empty NP, at doses of 10 to 50 μ g/mL.²⁴ Although chitosan is considered nontoxic and has been approved by the FDA for wound dressings, it has been shown to have antitumor effects on numerous human cancer cell lines *in vitro*.¹⁴ Its mechanism of action is to induce a robust IL-1 β response, via K⁺ efflux, formation of reactive oxygen species, and lysosomal destabilization.⁴² The mechanism by which NP causes dose-dependent cytotoxicity of both INS-R3 cells and murine islets is not clear from this study; further investigation in this area is warranted.

In contrast to previous studies, treatment with fBR had negligible protective effect on murine islets, and dose-dependent cytotoxicity was evident, although islets appeared to maintain insulin secretory function at doses of 5 to 10 μ M fBR. Doses of 25 to 50 μ M bilirubin have been found to interfere with mitochondrial respiration and induce necrosis and apoptosis of cells in culture.¹¹ The cytotoxicity of nBR at high doses in this study is therefore likely a result of the additive toxicity of bilirubin and the NP themselves. Although a larger number of intact islets were present following treatment with 10 μ M fBR than control, PI viability staining showed a higher percentage cell death in this group.

In conclusion, Pluronic F127–chitosan nanoencapsulation of bilirubin is feasible and results in improved cellular uptake via endocytosis in INS-R3 cells. In this *in vitro* investigation, dose-dependent protective effects of nBR on hypoxic murine islets were demonstrated, with doses of 5 μ M nBR providing maximum protective benefit, while preserving insulin secretory function. Treatment with 5 μ M nBR resulted in preservation of normal islet architecture, prevention of central necrosis, and improved islet function assessed by SI. Future work will focus on improving the efficiency of loading bilirubin into NP and the development of less cytotoxic NP for delivery of cytoprotective agents to transplanted cells.

Acknowledgments

The authors would like to thank Alice Harvey at NC State for her help in preparing the figures for the manuscript. We would also like to recognize Dr. John Bonagura at The Ohio State University and Dr. Emily Griffith at NC State for their guidance in the statistical analyses.

Ethical Approval

Experiments were approved by the Institutional Animal Care and Use Committee at The Ohio State University, protocol # 2012A0000121.

Statement of Human and Animal Rights

This study was carried out according to the National Research Council Guide for the Care and Use of Laboratory Animals.

Statement of Informed Consent

There are no human subjects in this article and informed consent is not applicable.

Declaration of Conflicting Interests

The author(s) declared no potential conflicts of interest with respect to the research, authorship, and/or publication of this article.

Funding

The author(s) disclosed receipt of the following financial support for the research and/or authorship of this article: This study was supported by a Paladin Award at The Ohio State University College of Veterinary Medicine (to C.A.A.)

References

1. Biarnés M, Montolio M, Nacher V, Raurell M, Soler J, Montanya E. Beta-cell death and mass in syngeneically transplanted islets exposed to short- and long-term hyperglycemia. *Diabetes*. 2002;51(1):66–72.
2. Kanak MA, Takita M, Kunnathodi F, Lawrence MC, Levy MF, Naziruddin B. Inflammatory response in islet transplantation. *Int J Endocrinol*. 2014;2014(6):1–13.
3. Matsuoka N, Itoh T, Watarai H, Sekine-Kondo E, Nagata N, Okamoto K, Mera T, Yamamoto H, Yamada S, Maruyama I, et al. High-mobility group box 1 is involved in the initial events of early loss of transplanted islets in mice. *J Clin Invest*. 2010; 120(3):735–743.
4. Adin CA, Croker BP, Agarwal A. Protective effects of exogenous bilirubin on ischemia-reperfusion injury in the isolated, perfused rat kidney. *Am J Physiol Renal Physiol*. 2004;288(4):F778–F784.
5. Adin CA, VanGundy ZC, Papenfuss TL, Xu F, Ghanem M, Lakey J, Hadley GA. Physiologic doses of bilirubin contribute to tolerance of islet transplants by suppressing the innate immune response. *Cell Transplant*. 2017;26(1):11–21.
6. Zhu H, Wang J, Jiang H, Ma Y, Pan S, Reddy S, Sun X. Bilirubin protects grafts against nonspecific inflammation-induced injury in syngeneic intraportal islet transplantation. *Exp Mol Med*. 2010;42(11):739–748.
7. Wang H, Lee SS, Dell'Agnello C, Tchpashvili V, D'Avilla J, Czismadia E, Chin BY, Bach FH. Bilirubin can induce tolerance to islet allografts. *Endocrinology*. 2006;147(2):762–768.

8. Zhu HQ, Gao Y, Guo HR, Kong QZ, Ma Y, Wang JZ, Pan SH, Jiang HC, Dai WJ. Pretreatment with bilirubin protects islet against oxidative injury during isolation and purification. *Transplant Proc.* 2011;43(5):1810–1814.
9. Kirkby KA, Adin CA. Products of heme oxygenase and their potential therapeutic applications. *Am J Physiol Renal Physiol.* 2005;290(3):F563–F571.
10. Keshavan P, Schwemberger SJ, Smith DLH, Babcock GF, Zucker SD. Unconjugated bilirubin induces apoptosis in colon cancer cells by triggering mitochondrial depolarization. *Int J Cancer.* 2004;112(3):433–445.
11. Khan NM, Poduval TB. Immunomodulatory and immunotoxic effects of bilirubin: molecular mechanisms. *J Leukoc Biol.* 2011;90(5):997–1015.
12. Zhang W, Gilstrap K, Wu L, K C RB, Moss MA, Wang Q, Lu X, He X. Synthesis and characterization of thermally responsive Pluronic F127–chitosan nanocapsules for controlled release and intracellular delivery of small molecules. *ACS Nano.* 2010;4(11):6747–6759.
13. Şenel S, McClure SJ. Potential applications of chitosan in veterinary medicine. *Adv Drug Deliv Rev.* 2004;56(10):1467–1480.
14. Wang JJ, Zeng ZW, Xiao RZ, Xie T, Zhou GL, Zhan XR, Wang SL. Recent advances of chitosan nanoparticles as drug carriers. *Int J Nanomedicine.* 2011;6:765–774.
15. Philippova OE, Korchagina EV. Chitosan and its hydrophobic derivatives: preparation and aggregation in dilute aqueous solutions. *Polym Sci Ser A.* 2012;54(7):552–572.
16. Rao W, Zhang W, Poventud-Fuentes I, Wang Y, Lei Y, Agarwal P, Weekes B, Li C, Lu X, Yu J, et al. Thermally responsive nanoparticle-encapsulated curcumin and its combination with mild hyperthermia for enhanced cancer cell destruction. *Acta Biomater.* 2014;10(2):831–842.
17. Lee KS, Gartner LM. Spectrophotometric characteristics of bilirubin. *Pediatr Res.* 1976;10(9):782–788.
18. Reed RG. Kinetics of bilirubin binding to bovine serum albumin and the effects of palmitate. *J Biol Chem.* 1977;252(21):7483–7487.
19. Erickson HP. Size and shape of protein molecules at the nanometer level determined by sedimentation, gel filtration, and electron microscopy. *Biol Proc Online.* 2009;11(1):32–51.
20. Glushko V, Thaler M, Ros M. The fluorescence of bilirubin upon interaction with human erythrocyte ghosts. *Biochim Biophys Acta.* 1982;719(1):65–73.
21. Zmuda EJ, Powell CA, Hai T. A method for murine islet isolation and subcapsular kidney transplantation. *J Vis Exp.* 2011; (50).
22. Zmuda EJ, Viapiano M, Grey ST, Hadley G, Garcia-Ocaña A, Hai T. Deficiency of Atf3, an adaptive-response gene, protects islets and ameliorates inflammation in a syngeneic mouse transplantation model. *Diabetologia.* 2010;53(7):1438–1450.
23. de Vargas LM, Sobolewski J, Siegel R, Moss LG. Individual beta cells within the intact islet differentially respond to glucose. *J Biol Chem.* 1997;272(42):26573–26577.
24. Ghosh K, Kanapathipillai M, Korin N, McCarthy JR, Ingber DE. Polymeric nanomaterials for islet targeting and immunotherapeutic delivery. *Nano Lett.* 2012;12(1):203–208.
25. Giuliani M, Moritz W, Bodmer E, Dindo D, Kugelmeier P, Lehmann R, Gassmann M, Groscurth P, Weber M. Central necrosis in isolated hypoxic human pancreatic islets: evidence for postisolation ischemia. *Cell Transplant.* 2005;14(1):67–76.
26. Singh R, Lillard JW Jr. Nanoparticle-based targeted drug delivery. *Exp Mol Pathol.* 2009;86(3):215–223.
27. Xiong XY, Tam KC, Gan LH. Release kinetics of hydrophobic and hydrophilic model drugs from pluronic F127/poly(lactic acid) nanoparticles. *J Control Release.* 2005;103(1):73–82.
28. Modi S, Anderson BD. Determination of drug release kinetics from nanoparticles: overcoming pitfalls of the dynamic dialysis method. *Mol Pharm.* 2013;10(8):3076–3089.
29. Das RK, Kasoji N, Bora U. Encapsulation of curcumin in alginate-chitosan-pluronic composite nanoparticles for delivery to cancer cells. *Nanomedicine.* 2010;6(1):153–160.
30. Zunszain PA, Ghuman J, McDonagh AF, Curry S. Crystallographic analysis of human serum albumin complexed with 4Z,15E-Bilirubin-IX α . *J Mol Biol.* 2008;381(2):394–406.
31. De Jong WH, Borm PJ. Drug delivery and nanoparticles: applications and hazards. *Int J Nanomed.* 2008;3(2):133–149.
32. Orci L, Malaisse-Lagae F, Ravazzola M, Amherdt M, Renold AE. Exocytosis-endocytosis coupling in the pancreatic beta cell. *Science.* 1973;181(4099):561–562.
33. Panyam J, Zhou WZ, Prabha S, Sahoo SK, Labhasetwar V. Rapid endo-lysosomal escape of poly (DL-lactide-co-glycolide) nanoparticles: implications for drug and gene delivery. *FASEB J.* 2002;16(10):1217–1226.
34. Yang YHC, Johnson JD. Multi-parameter single-cell kinetic analysis reveals multiple modes of cell death in primary pancreatic -cells. *J Cell Sci.* 2013;126(18):4286–4295.
35. Frank LA, Contri RV, Beck RCR, Pohlmann AR, Guterres SS. Improving drug biological effects by encapsulation into polymeric nanocapsules. *Wiley Interdiscip Rev Nanomed Nanobio-technol.* 2015;7(5):623–639.
36. Steiner DJ, Kim A, Miller K, Hara M. Pancreatic islet plasticity. *Islets.* 2010;2(3):135–145.
37. Carter JD, Dula SB, Corbin KL, Wu R, Nunemaker CS. A practical guide to rodent islet isolation and assessment. *Biol Proc Online.* 2009;11(1):3–31.
38. Sakata N, Egawa S, Sumi S, Unno M. Optimization of glucose level to determine the stimulation index of isolated rat islets. *Pancreas.* 2008;36(4):417–423.
39. Komatsu M, Takei M, Ishii H, Sato Y. Glucose-stimulated insulin secretion: a newer perspective. *J Diabetes Invest.* 2013;4(6):511–516.
40. Goto M, Holgersson J, Kumagai-Braesch M, Korsgren O. The ADP/ATP ratio: a novel predictive assay for quality assessment of isolated pancreatic islets. *Am J Transplant.* 2006; 6(10):2483–2487.
41. Suszynski TM, Wildey GM, Falde EJ, Cline GW, Maynard KS, Ko N, Sotiris J, Naji A, Hering BJ, Papas KK. The ATP/DNA ratio is a better indicator of islet cell viability than the ADP/ATP ratio. *Transplant Proc.* 2008;40(2):346–350.
42. Bueter CL, Lee CK, Wang JP, Ostroff GR, Specht CA, Levitz SM. Spectrum and mechanisms of inflammasome activation by chitosan. *J Immunol.* 2014;192(12):5943–5951.